

Photodissociation Spectroscopy and Dissociation Dynamics of $\text{TiO}^+(\text{CO}_2)$

K. Manori Perera and Ricardo B. Metz*

Department of Chemistry, University of Massachusetts Amherst, Amherst, Massachusetts 01003

Received: October 31, 2008; Revised Manuscript Received: March 25, 2009

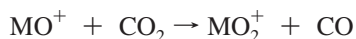
$\text{TiO}^+(\text{CO}_2)$ is produced by reaction of laser-ablated titanium atoms with CO_2 and subsequent clustering, supersonically cooled, and its electronic spectroscopy was characterized by photofragment spectroscopy, monitoring loss of CO_2 . The photodissociation spectrum consists of a vibrationally resolved band in the visible, with extensive progressions in the covalent Ti–O stretch (952 cm^{-1} vibrational frequency and 5 cm^{-1} anharmonicity) and in the TiO^+-CO_2 stretch (186 cm^{-1}) and rock (45 cm^{-1}). The band origin is at $13\,918\text{ cm}^{-1}$, assigned using titanium isotope shifts, and the spectrum extends to $17\,350\text{ cm}^{-1}$. The excited-state lifetime decreases dramatically with increasing internal energy, from 1100 ns for the lowest energy band ($v'_{\text{TiO}} = 0$) to $<50\text{ ns}$ for $v'_{\text{TiO}} = 3$. The long photodissociation lifetime substantially reduces the photodissociation quantum yield at low energy, likely due to competition with fluorescence. The fluorescence rate is calculated to be $k_{\text{fl}} = 7.5 \times 10^5\text{ s}^{-1}$, based on the measured excited-state lifetimes and relative band intensities. This corresponds to an integrated oscillator strength of $f = 0.0056$. Electronic structure calculations help to assign the spectrum of $\text{TiO}^+(\text{CO}_2)$ and predict allowed electronic transitions of TiO^+ in the visible, which have not been previously measured. Time-dependent density functional calculations predict that the observed transition is due to $\text{B}, {}^2\Pi \leftarrow \text{X}, {}^2\Delta$ in the TiO^+ chromophore and that binding to CO_2 red shifts the TiO^+ transition by 1508 cm^{-1} and lowers the Ti–O stretch frequency by 16 cm^{-1} . Combining the computational and experimental results, the ${}^2\Pi$ state of TiO^+ is predicted to lie at $T_0 = 15\,426 \pm 200\text{ cm}^{-1}$, with frequency $\omega_e = 968 \pm 5\text{ cm}^{-1}$ and anharmonicity $\omega_e x_e = 5\text{ cm}^{-1}$. The calculations also predict that there is only one low-lying ${}^2\Sigma$ state of TiO^+ , contrary to conclusions derived from photoelectron spectroscopy of TiO . Prospects for astronomical observation of TiO^+ via the ${}^2\Pi-{}^2\Delta$ transition are also discussed.

I. Introduction

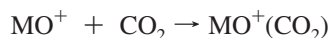
One of the most important applications of transition metal oxides is as heterogeneous catalysts.^{1,2} As a result, there have been many studies of gas-phase metal oxide cations to understand the oxo ligand influence on metal chemistry and to characterize reactions such as methane to methanol conversion.^{3–10} Bare Ti^+ is very oxophilic, reacting exothermically with water and O_2 to produce TiO^+ .^{11–13} Recently, Koyanagi and Böhme¹⁴ and Herman et al.¹⁵ measured the room temperature kinetics of the sequential reactions of 46 main group and transition metal cations with CO_2 . Several early transition metal cations (including Ti^+) activate CO_2 :



Sequential activation is observed for Hf^+ , Nb^+ , Ta^+ , and W^+ :



Breaking the OC–O bond requires 533 kJ/mol. Thus, Ti^+ oxygen abstraction from CO_2 is consistent with the measured Ti^+-O bond strength of $664 \pm 7\text{ kJ/mol}$.^{16,17} In the presence of helium buffer gas, many metal oxides, including TiO^+ , cluster with CO_2 .^{14,15}



Due to interest in CO_2 activation, the electronic and vibrational spectroscopy of several transition metal cation complexes with CO_2 have been measured. This includes studies of the electronic

spectroscopy of $\text{Ni}^+(\text{CO}_2)$ and $\text{Co}^+(\text{CO}_2)$ by Brucat and co-workers,^{18–20} of the electronic and vibrational spectroscopy of $\text{V}^+(\text{CO}_2)$ in our group,^{21,22} and of the vibrational spectroscopy of $\text{M}^+(\text{CO}_2)_n$ clusters for several metals by Duncan and co-workers.^{23–26}

Other studies have focused on $\text{MO}^+(\text{CO}_2)$ to understand metal–ligand interactions. Bellert et al. produced $\text{ZrO}^+(\text{CO}_2)$ using molecular-beam methods and probed an excited electronic state with photofragment spectroscopy.²⁷ Vibrational structure in the photodissociation spectrum characterizes noncovalent interactions between CO_2 and electronically excited ZrO^+ . Binding to CO_2 decreases the energy gap to the excited state, indicating that the solvent molecule binds to the excited state much more strongly than to the ground state. This can be explained with respect to the upper electronic state properties of ZrO^+ , particularly the greater electric dipole moment and increased bond length. Similar results are obtained for $\text{ZrO}^+(\text{N}_2)$.

Transition metal oxides are also interesting due to their importance in astronomy. The TiO molecule dominates the absorption opacity of M-type stars in the visible and near-infrared regions.^{28,29} TiO absorptions are used for spectral classification of cool M and S class stars,³⁰ and the temperature of the stellar atmosphere can be determined from the rotational, vibrational, and spin–orbit structure of these bands.^{31,32} Due to the low ionization energy of Ti (658.8 kJ/mol)³³ and very high Ti^+-O bond strength ($664 \pm 7\text{ kJ/mol}$),^{16,17} TiO^+ can be produced via associative ionization (chemiionization):^{34–36}



This reaction is also an important source of free electrons in interstellar clouds, due to the relatively high abundance of

* To whom correspondence should be addressed. E-mail: rbmetz@chemistry.umass.edu.

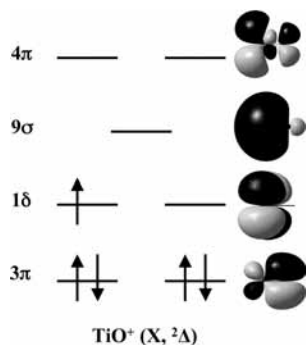


Figure 1. Molecular orbital diagram and electron occupancy of TiO^+ ($X, {}^2\Delta$).

titanium.^{37,38} Hence, studying the ground and excited electronic states of TiO and TiO^+ in a quantitative manner is very important. There have been numerous spectroscopic^{39–43} and computational^{28,44} studies of TiO . In contrast, the electronic spectroscopy of TiO^+ has not been measured, and there have been few computational studies.

To date, the only spectroscopic information on TiO^+ is from photoelectron spectroscopy of TiO . Dyke et al.⁴⁵ irradiated TiO from a high-temperature oven with 21.22 eV photons and observed transitions assigned to two states of TiO^+ . A weak band due to ionization to TiO^+ ($X, {}^2\Delta$) gives an ionization energy of 6.82 ± 0.02 eV. A second band at $T_0 = 10\,250 \pm 80$ cm^{-1} with vibrational frequency $\omega_e = 860 \pm 60$ cm^{-1} and $r_e = 1.73 \pm 0.01$ Å was assigned to the $A, {}^2\Sigma^+$ state. Neutral TiO has a ${}^3\Delta$ ground state with the electron configuration $\dots 8\sigma^2, 3\pi^4, 1\delta^1, 9\sigma^1$ and $r_e = 1.620$ Å. The ${}^2\Delta$ ground state of TiO^+ results from removing the 9σ electron (Figure 1). Removing the 1δ electron produces the ${}^2\Sigma$ excited state. Sappey et al. measured the photoelectron spectrum of supersonically cooled TiO using resonance-enhanced multiphoton ionization.⁴⁶ They measured an ionization energy of 6.819 ± 0.006 eV. This is in excellent agreement with the earlier photoelectron result and the value of 6.8197 ± 0.0007 eV obtained by Look et al.⁴⁷ using two-color photoionization efficiencies and mass-analyzed threshold ionization. The vibrational frequency of the TiO^+ ground state is $\omega_e = 1045 \pm 7$ cm^{-1} , with anharmonicity $\omega_e x_e = 4 \pm 1$ cm^{-1} . They observe an excited ${}^2\Sigma^+$ state with an origin at $11\,227 \pm 17$ cm^{-1} , vibrational frequency $\omega_e = 1020 \pm 9$ cm^{-1} , and anharmonicity $\omega_e x_e = 6 \pm 2$ cm^{-1} . Although this state lies at a similar energy to the ${}^2\Sigma$ observed by Dyke and co-workers, the very different vibrational frequencies led Weisshaar and co-workers to propose that TiO^+ has two distinct low-lying ${}^2\Sigma$ states, and resonant two-photon ionization reaches one state, while one-photon ionization reaches another. Unfortunately, ${}^2\Delta$ – ${}^2\Sigma$ optical transitions are forbidden, so these states are difficult to characterize by electronic spectroscopy of TiO^+ and are not useful for astronomical observation of TiO^+ .

The Ti^+ –O bond is very strong, and consequently, it is difficult to use photofragment spectroscopy to observe the absorptions of this molecule. To understand the excited states without breaking the Ti^+ –O bond, one can attach a spy molecule like CO_2 and then break the metal–ligand bond. We measured the photodissociation spectrum of $\text{TiO}^+(\text{CO}_2)$ to characterize an excited state of the TiO^+ chromophore. When TiO^+ is photoexcited, its electron density changes and the response of the ligand to these changes is reflected in the photodissociation spectrum. In addition, calculations help to further characterize the ground and excited states of TiO^+ and $\text{TiO}^+(\text{CO}_2)$.

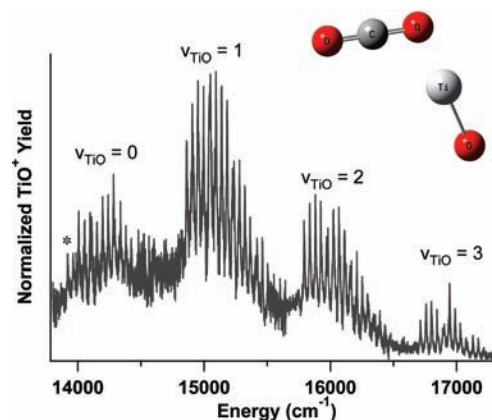


Figure 2. Photodissociation spectrum of $\text{TiO}^+(\text{CO}_2)$ with the covalent Ti –O stretch vibrational quantum numbers ν_{TiO} marked. The asterisk denotes the electronic state origin. The inset shows the geometry of $\text{TiO}^+(\text{CO}_2)$ calculated at the B3LYP/6-311+G(d) level.

II. Experimental Approach

The experimental apparatus, a dual time-of-flight reflectron photofragment spectrometer, and methods used have been described in detail previously.^{48–50} In this study, titanium cations are generated by laser ablation of a translating and rotating titanium rod (Strem Chemicals, 99.98% pure). The Ti^+ ions react with $\sim 0.1\%$ carbon dioxide (99.98% pure) seeded in helium introduced through a piezoelectric pulsed valve to produce TiO^+ and $\text{TiO}^+(\text{CO}_2)_n$. The ions in the plasma undergo supersonic expansion into vacuum, leading to substantial cooling. Vibrationally mediated photodissociation of $\text{V}^+(\text{CO}_2)$ reveals a rotational temperature of 12 K for ions produced in this source.²¹ The ion beam is skimmed, extracted into the time-of-flight mass spectrometer, and referenced to ground potential. The mass-selected ions of interest are photoexcited at the turning point of the reflectron by the output of a pulsed (20 Hz) Nd:YAG-pumped dye laser with a line width of <0.1 cm^{-1} . Fragment and parent ions reaccelerate to a dual-microchannel-plate detector. The resulting signal is amplified, collected on a digital oscilloscope or a gated integrator, and recorded digitally using a LabView-based program. The photofragment experiments produce two types of spectra. *Difference spectra* are obtained by subtracting time-of-flight spectra with the dissociation laser blocked from those with it unblocked. Difference spectra are used to identify fragment ions and their relative abundance at a given wavelength. The difference spectrum can also give information on the dissociation dynamics and kinetics. Kinetic energy release leads to broadening of the fragment time-of-flight peaks, while slow dissociation leads to tailing in the fragment peak toward the parent time.⁵¹ *Photodissociation spectra* are obtained by monitoring the fragment ion yield as a function of wavelength and normalizing to the parent ion signal and laser power. The intensities of features in the photodissociation spectrum are proportional to the product of the absorption cross section and the quantum yield for photodissociation.

III. Results and Discussion

A. Photodissociation Spectroscopy and Dissociation Kinetics of $\text{TiO}^+(\text{CO}_2)$. The photodissociation spectrum provides the absorption spectrum of $\text{TiO}^+(\text{CO}_2)$ when absorption leads to dissociation. Figure 2 shows the resonant photodissociation spectrum of ${}^{48}\text{TiO}^+(\text{CO}_2)$ obtained by monitoring ${}^{48}\text{TiO}^+$, the only fragment observed. The spectrum is richly structured, with four bands separated by ~ 950 cm^{-1} ; each band consists of

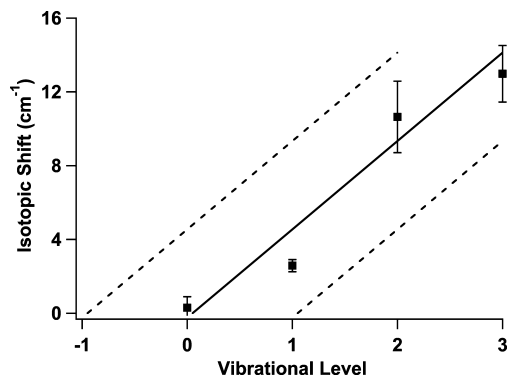


Figure 3. Assignment of covalent Ti–O stretch vibrational levels v_{TIO} in the photodissociation spectrum of $\text{TiO}^+(\text{CO}_2)$. Experimental isotope shifts are compared to calculated shifts assuming the vibrational numbering is as shown in Figure 2 (solid line) and with the numbering shifted by one (dashed lines).

several peaks separated by $\sim 50 \text{ cm}^{-1}$. In order to identify the vibrational progressions in the electronic spectrum of $\text{TiO}^+(\text{CO}_2)$ we first consider the vibrational frequencies of TiO^+ and CO_2 . The vibrational frequency⁴⁶ of the TiO^+ ground state is $\omega_e = 1045 \pm 7 \text{ cm}^{-1}$, with anharmonicity $\omega_{e x_e} = 4 \pm 1 \text{ cm}^{-1}$; the vibrational frequencies of CO_2 are 2349, 1333, and 667 cm^{-1} . The $\sim 950 \text{ cm}^{-1}$ progression observed is thus likely due to the covalent Ti–O stretch in the excited state of $\text{TiO}^+(\text{CO}_2)$, while the low-frequency vibration(s) are due to noncovalent metal– CO_2 stretches and bends. In order to confirm the assignment of the high-frequency progression and to establish vibrational quantum numbers we measure the photodissociation spectrum of $\text{TiO}^+(\text{CO}_2)$ using the minor ^{50}Ti isotope (5% natural abundance), rather than ^{48}Ti (74% abundance). Since vibrational frequencies depend on the reduced mass of the molecule, the Ti–O⁺ stretching frequency of the heavier $^{50}\text{TiO}^+$ isotopomer is lower than that of the more abundant $^{48}\text{TiO}^+$ isotopomer. Ignoring anharmonicity and the influence of the CO_2 , the ratio of reduced masses yields $\omega_{50} = 0.994986 \omega_{48}$. Using the vibrational frequencies of the ground (1045 cm^{-1}) and excited (950 cm^{-1}) states of TiO^+ gives an isotopic shift (in cm^{-1}) of

$$E_{48\text{TiO}^+} - E_{50\text{TiO}^+} \approx 4.76v' - 0.24 \quad (1)$$

where v' is the excited state vibrational quantum number. Figure 3 shows the measured isotopic shifts, and the predictions of eq 1 for the cases where the first observed band corresponds to $v' = 0$ (best fit), $v' = 1$, and where the second band is due to $v' = 0$. With the vibrational numbering established, the peak at 13918 cm^{-1} (asterisk in Figure 2) is the origin. The excited state covalent TiO^+ stretching frequency is $\omega'_{\text{TIO}} = 952 \text{ cm}^{-1}$ with anharmonicity $x'_{\text{TIO}} = 5 \text{ cm}^{-1}$.

Figure 4 again shows the photodissociation spectrum of $\text{TiO}^+(\text{CO}_2)$ but with the four high-frequency bands shifted to allow for better comparison of the low-frequency structure in each band. The four bands exhibit almost identical low-frequency structure, indicating that there is little coupling between the covalent Ti–O stretch and the metal– CO_2 stretches and bends. There are progressions in two low-frequency modes: at 45 and 186 cm^{-1} . The 186 cm^{-1} vibration is assigned to the noncovalent metal– CO_2 stretch, while the lowest frequency vibration is due to the metal– CO_2 rock. Every fourth peak is split, as the stretch frequency is not quite an integer multiple of the rocking frequency. The long progressions observed in the metal–ligand rock and, to a lesser extent, stretch indicate that the TiO^+ electronic state substantially affects its interaction with CO_2 . This will be explored in more detail with the aid of

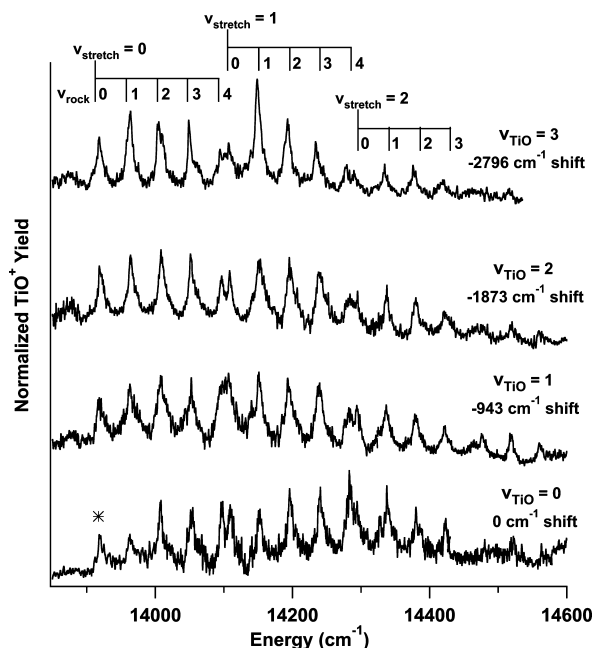


Figure 4. Overlapped photodissociation spectrum of $\text{TiO}^+(\text{CO}_2)$. Bands corresponding to the covalent Ti–O stretch $v_{\text{TIO}} = 0-3$ are shifted to allow comparison of the low-frequency metal– CO_2 stretch and rock. The low-frequency vibrations are essentially independent of v_{TIO} . The asterisk denotes the electronic state origin.

electronic structure calculations. It is also interesting to compare the photodissociation spectrum of $\text{TiO}^+(\text{CO}_2)$ to that of iso-electronic $\text{ZrO}^+(\text{CO}_2)$ obtained by Bellert et al.²⁷ The spectra are very similar. They observe a progression in the Zr–O covalent stretch ($\omega'_{\text{ZrO}} = 891 \text{ cm}^{-1}$, $x'_{\text{ZrO}} = 3.4 \text{ cm}^{-1}$), as well as the metal– CO_2 stretch ($\omega'_{\text{stretch}} = 173 \text{ cm}^{-1}$) and rock ($\omega'_{\text{rock}} = 39 \text{ cm}^{-1}$). These values are very similar to those we observe for $\text{TiO}^+(\text{CO}_2)$. The titanium complex does, however, show a more extensive progression in the rock, indicating that electronic excitation of TiO^+ results in a larger change in the orientation of the CO_2 ligand.

The shape of the fragment peak in the time-of-flight spectrum is sensitive to dissociation dynamics and kinetics. Substantial kinetic energy release leads to peak broadening, while slow dissociation leads to peak tailing.⁵¹ Figure 5 shows the TiO^+ fragment peak from photodissociation of $\text{TiO}^+(\text{CO}_2)$ at 14204 and 14925 cm^{-1} . The 14204 cm^{-1} spectrum shows clear tailing, which is much reduced at 14925 cm^{-1} . The lifetimes of the photoexcited molecules are determined by comparing experimental and simulated⁵¹ fragment time-of-flight profiles. Excited state lifetimes measured at several photon energies covering $v_{\text{TIO}} = 0-3$ are shown in Table 1. The lifetime drops rapidly with increasing photon energy, until no tailing is observed at energies above 16500 cm^{-1} , indicating lifetimes below 50 ns.

B. Calculations. Electronic structure calculations were carried out on TiO^+ and $\text{TiO}^+(\text{CO}_2)$ to determine which state of the TiO^+ chromophore is responsible for the observed spectrum, as well as to investigate the photodissociation mechanism and the broad range of dissociation lifetimes. In addition, by calculating how the CO_2 affects the vibrational frequencies and electronic spectroscopy of TiO^+ , we can use our experimental results on $\text{TiO}^+(\text{CO}_2)$ to predict the electronic spectrum of bare TiO^+ in the visible. Calculations were carried out using the B3LYP hybrid density functional method, with the 6-311+G(d) basis set, using Gaussian03.⁵² At this level of theory, bare TiO^+ is predicted to have a ${}^2\Delta$ ground state, with the electron configuration $\dots 8\sigma^2, 3\pi^4, 1\delta^1$ and $r_e = 1.570 \text{ \AA}$. To characterize

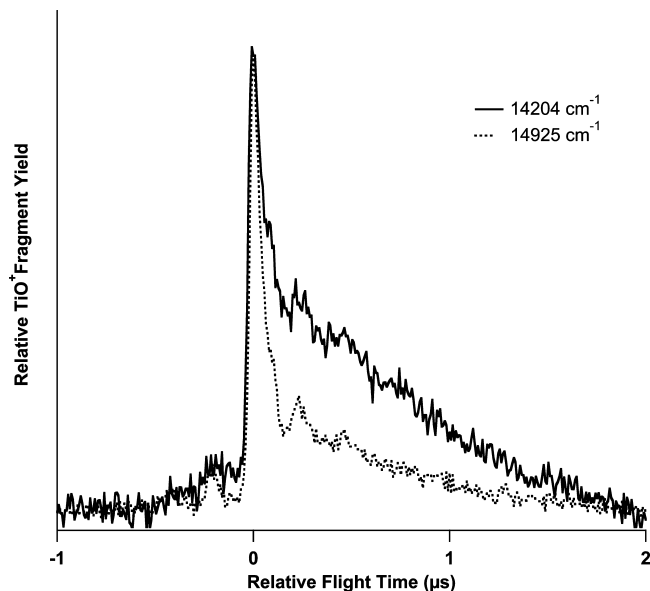


Figure 5. Time-of-flight spectra of TiO^+ from photodissociation of $\text{TiO}^+(\text{CO}_2)$ at 14 204 and 14 925 cm^{-1} . Tailing in the 14 204 cm^{-1} spectrum indicates a lifetime of 1100 ns, which drops to 120 ns at 14 925 cm^{-1} . The small peaks in the spectra are due to photodissociation of minor isotopomers.

TABLE 1: Excited-State Lifetimes and Excited-State Decay Rates for Several Vibronic States of $\text{TiO}^+(\text{CO}_2)^a$

energy (cm^{-1})	lifetime, τ (ns)	rate, $1/\tau$ (s^{-1})
14 204	1100	9×10^5
14 925	120	8×10^6
15 798	60	1.7×10^7
16 722	≤ 50	$\geq 2 \times 10^7$

^a The lifetimes are measured from fits to tailing in the TiO^+ fragment time-of-flight spectrum, as shown in Figure 5.

excited electronic states, time-dependent density functional theory (TD-DFT) calculations were carried out at the B3LYP/6-311+G(d) level. Because Gaussian03 does not have the capability to optimize TD-DFT excited state geometries, this optimization was done manually, by scanning along each internal coordinate. There are two low-lying excited states: the $^2\Sigma$ state is formed by promotion of the 1δ electron to the 9σ orbital (see Figure 1); promotion to the 4π orbital produces the $^2\Pi$ state. Figure 6 shows scans along the Ti–O stretch for the ground and low-lying doublet states of TiO^+ . The low-lying $^2\Sigma$ and $^2\Pi$ states have similar energies at $r > 1.8 \text{ \AA}$, as they both correlate to Ti^+ ($a, ^4F$) + O (3P), as do the ground and several excited states, including a second $^2\Sigma$ state, discussed below. Spectroscopic parameters obtained by solving the Schrödinger equation for the one-dimensional stretching potential are given in Table 2. Transitions from the $^2\Delta$ ground state to the $^2\Sigma$ excited state are forbidden. Transitions to the $^2\Pi$ state are calculated to have an integrated oscillator strength $f = 0.0050$.

Several groups have carried out calculations on TiO^+ using density functional and correlated ab initio methods. The doublet ground state and lowest quartet state of TiO^+ were characterized in surveys of metal–oxide bonding trends^{53,54} and in studies of the $\text{Ti}^+ + \text{H}_2\text{O}$ and $\text{Ti}^+ + \text{CO}_2$ reactions.^{15,55,56} However, these studies did not characterize excited doublet states of TiO^+ . As part of a study of Rydberg states of TiO , McLaughlin et al.⁵⁷ calculated excited doublet states of TiO^+ . They obtain slightly higher excitation energies to the $^2\Sigma$ and $^2\Pi$ than our TD-DFT results, likely due to their use of a small Slater-type basis set.

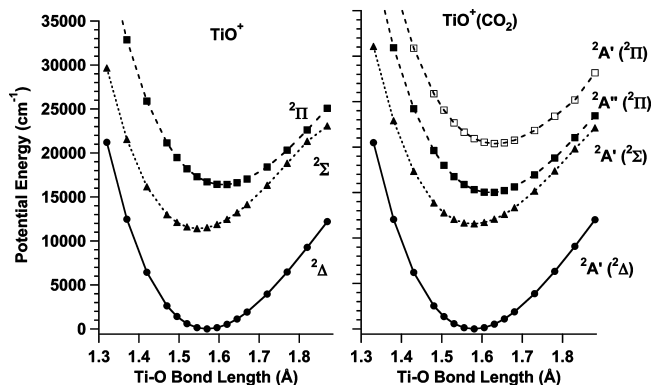


Figure 6. Calculated potential-energy curves for doublet states of TiO^+ and $\text{TiO}^+(\text{CO}_2)$ along the covalent Ti–O stretch. Points are calculated using TD-DFT at the B3LYP/6-311+G(d) level. Electronic states of $\text{TiO}^+(\text{CO}_2)$ are also labeled by the corresponding state of bare TiO^+ . The $^2A''(^2\Pi)$ state of $\text{TiO}^+(\text{CO}_2)$ is not shown, as it is nearly degenerate with the $^2A'(^2\Delta)$ state.

TABLE 2: Spectroscopic Parameters for the Ground and Low-Lying Excited States of TiO^+ from TD-DFT Calculations at the B3LYP/6-311+G(d) Level^a

state	r_c (\AA)	ω_e (cm^{-1})	ω_{ex_e} (cm^{-1})	T_e (cm^{-1})	T_0 (cm^{-1})
$^2\Delta$, harmonic	1.570	1122.1	0	0	0
$^2\Delta$	1.570	1122.5	4.18	0	0
$^2\Sigma$	1.548	1130.9	4.84	11 399	11 403
$^2\Pi$	1.610	1049.6	3.89	16 385	16 348

^a The first row is an analytical harmonic frequency. Other rows are anharmonic frequencies from the potentials in Figure 6.

Miliordos and Mavridis⁵⁸ carried out a series of very high-level calculations on the ground and excited electronic states of TiO and TiO^+ . Their highest level calculations are multireference configuration interaction, with quadruple excitations estimated via the Davidson correction, and scalar relativistic effects included by the second-order Douglas–Kroll–Hess method (C-MRCI+Q+DKH2).⁵⁹ At this level of theory, they predict $\omega_e = 1059$ and $\omega_{ex_e} = 4.7 \text{ cm}^{-1}$ for the ground state and that the $^2\Sigma$ and $^2\Pi$ states lie at $T_e = 10 700$ and $15 400 \text{ cm}^{-1}$, respectively, with frequencies of $\omega_e = 1032$ and $\omega_{ex_e} = 4.8 \text{ cm}^{-1}$ ($^2\Sigma$) and $\omega_e = 969$ and $\omega_{ex_e} = 4.4 \text{ cm}^{-1}$ ($^2\Pi$). Our TD-DFT calculations are in excellent agreement with the multireference calculations with respect to geometries and excitation energies, although the calculated frequencies are about 8% too high. This is consistent with TD-DFT calculations on other transition metal oxide cations, which predict excitation energies with mean errors of 2000 cm^{-1} .^{49,60}

The geometry of $\text{TiO}^+(\text{CO}_2)$ calculated at the B3LYP/6-311+G(d) level is shown in Figure 2. The complex is planar. Binding to CO_2 lengthens the covalent Ti–O bond by 0.010 \AA , to 1.580 \AA . The noncovalent OTi–OCO bond length is 2.19 \AA , and the complex is bent, with an OTi–(OCO) angle of 107° . The CO_2 is bound by 8000 cm^{-1} . Figure 6 shows scans of doublet states of $\text{TiO}^+(\text{CO}_2)$ along the covalent Ti–O stretch. Interaction with CO_2 lowers the symmetry of the $^2\Delta$ ground state of TiO^+ , resulting in two, nearly degenerate states ($^2A'$ is slightly lower than $^2A''$). Interaction with CO_2 leads to much larger splitting for the $^2\Pi$ excited state of TiO^+ . The lower energy $^2A''(^2\Pi)$ component corresponds to an electron in the out-of-plane π orbital, resulting in less repulsion with CO_2 than promotion to the in-plane π orbital. The $^2A''(^2\Pi)$ state retains significant oscillator strength ($f = 0.0057$), while the $^2A'$ component has $f \approx 0$. As for the low-lying $^2\Sigma$ state of TiO^+ , binding to CO_2 lowers the symmetry, so transitions to the $^2A'$

TABLE 3: Spectroscopic Parameters for the Covalent Ti–O Stretch in the Ground and Low-Lying Excited States of $\text{TiO}^+(\text{CO}_2)$ from TD-DFT Calculations at the B3LYP/6-311+G(d) Level^a

state	ω_e (cm ⁻¹)	$\omega_e x_e$ (cm ⁻¹)	T_e (cm ⁻¹)	T_0 (cm ⁻¹)
2A' (² Δ), harmonic	1106	0	0	0
2A' (² Δ)	1103.5	3.16	0	0
2A' (² Σ)	1062.4	3.31	11 552	11 531
2A'' (² Π)	1033.5	3.96	14 992	14 957

^aThe first row is a harmonic frequency. Other rows are anharmonic frequencies from the potentials in Figure 6. Electronic states of $\text{TiO}^+(\text{CO}_2)$ are also labeled by the corresponding state of bare TiO^+ in parentheses. Interaction with CO_2 splits the ²Π state into two components. Parameters are not given for the upper 2A' (²Π) state.

TABLE 4: Calculated Vibrational Frequencies of $\text{TiO}^+(\text{CO}_2)$ at the B3LYP/6-311+G(d) Level

assignment	frequency (cm ⁻¹)
CO ₂ antisymmetric stretch	2458
CO ₂ symmetric stretch	1377
CO ₂ bend	639 and 647
covalent Ti–O stretch	1106
OTi–(OCO) stretch	255
OTi–(OCO) rock	53, 100, and 132

(²Σ) state are no longer forbidden but are weak with $f = 0.0007$. Calculated spectroscopic parameters for the covalent Ti–O stretch in $\text{TiO}^+(\text{CO}_2)$ are given in Table 3. Calculated harmonic vibrational frequencies for the ground state of $\text{TiO}^+(\text{CO}_2)$ are in Table 4.

C. Discussion. The photodissociation spectrum of $\text{TiO}^+(\text{CO}_2)$ has an origin at 13 918 cm⁻¹ and shows extensive progressions in the covalent Ti–O stretch ($\omega'_{\text{TiO}} = 952$ cm⁻¹ with anharmonicity $x'_{\text{TiO}} = 5$ cm⁻¹) and the metal–CO₂ stretch and rock (186 and 45 cm⁻¹, respectively). The calculations predict two states of $\text{TiO}^+(\text{CO}_2)$ in this region: the 2A' (²Σ) and 2A'' (²Π) states. Transitions to the 2A' (²Σ) state are predicted to be about an order of magnitude weaker than those to the 2A'' (²Π) state. Since we observe only one electronic transition, it is assigned to the 2A'' (²Π) state, and this assignment is consistent with a drop in the Ti–O stretching frequency on photoexcitation. The calculations predict that this state is at an adiabatic energy of $T_e = 14 877$ cm⁻¹, if the excited state geometry is optimized along all coordinates. Photoexcitation of $\text{TiO}^+(\text{CO}_2)$ to this state is calculated to increase the covalent Ti–O bond length by 0.04 Å, decrease the OTi–OCO bond length by 0.04 Å, and decrease the O–Ti–OCO angle by 13°. These geometry changes would lead to short progressions in the covalent Ti–O stretch and the metal–CO₂ stretch and an extensive progression in the rock, as observed. The calculation slightly overestimates the covalent TiO stretch frequency, predicting $\omega'_{\text{TiO}} = 1033.5$ cm⁻¹ with anharmonicity $x'_{\text{TiO}} = 4$ cm⁻¹. The calculations predict that TiO^+ (X, ²Δ) binds CO₂ by 8000 cm⁻¹. The calculated 1508 cm⁻¹ red shift for excitation to the 2A' (²Π) state indicates that the ²Π state of TiO^+ binds CO₂ more strongly, by ~9500 cm⁻¹. This stronger interaction is also consistent with the calculated reduction in the OTi–OCO bond length upon photoexcitation. Despite this strong binding, interaction with the CO₂ only slightly affects the vibrational frequency of TiO^+ , reducing it by 16 cm⁻¹ according to the calculations.

The wide range of excited state lifetimes observed for $\text{TiO}^+(\text{CO}_2)$ is unusual for a molecule this small. Photoexcitation of $\text{TiO}^+(\text{CO}_2)$ initially produces $[\text{TiO}^+(\text{CO}_2)]^*$ 2A'' (²Π). Dissociation requires internal conversion or intersystem crossing

to a lower lying electronic state followed by intermolecular vibrational relaxation (IVR) to transfer sufficient energy to the OTi–OCO stretch to dissociate the complex. Intersystem crossing does not contribute since the lowest quartet state is calculated to lie above the photon energy. We can use a statistical model to predict whether internal conversion or IVR is the rate-limiting step. If internal conversion of $[\text{TiO}^+(\text{CO}_2)]^*$ to highly vibrationally excited $\text{TiO}^+(\text{CO}_2)$ in its ground electronic state is rapid, then the statistical RRKM model can be used to predict the unimolecular dissociation rate of the energized complex. Using computed vibrational frequencies (Table 4) and the calculated TiO^+ –CO₂ binding energy of 8000 cm⁻¹, the statistical dissociation rate is 3×10^{10} s⁻¹ at a photon energy of 14 000 cm⁻¹. Increasing the binding energy to 10 000 cm⁻¹ only drops the dissociation rate is 3×10^9 at 14 000 cm⁻¹. This is over 3 orders of magnitude faster than is observed. Thus, these calculations predict that IVR is rapid and internal conversion is the rate-limiting step. The observed intensities in the photodissociation spectrum (Figure 2) provide further evidence that the 2A'' (²Π) state of $\text{TiO}^+(\text{CO}_2)$ is sufficiently long lived that fluorescence competes with predissociation. Using the potentials in Figure 6 for the 2A' (²Δ) and 2A'' (²Π) states of $\text{TiO}^+(\text{CO}_2)$, absorption to the $v_{\text{TiO}} = 0; v_{\text{TiO}} = 1$ peaks should have an intensity ratio of 1:0.3. This is quite different from the intensities in the photodissociation spectrum, which are in a ratio of ~0.6:1. This implies that the photodissociation quantum yield Φ_d for the $v_{\text{TiO}} = 0$ band is only 18% that for the $v_{\text{TiO}} = 1$ band. As Table 1 shows, the excited state lifetime for the $v_{\text{TiO}} = 0$ band is about an order of magnitude larger than for the $v_{\text{TiO}} = 1$ band. This suggests that fluorescence competes with photodissociation. The photodissociation quantum yields and the observed excited state decay rates (Table 1) can be used to estimate the fluorescence rate and the oscillator strength. Assuming that the $v_{\text{TiO}} = 0$ and 1 bands have the same fluorescence rate and that only fluorescence and dissociation contribute to the excited state decay rate, the fluorescence rate is $k_f = 7.5 \times 10^5$ s⁻¹. This implies an integrated oscillator strength of $f = 0.0056$. The agreement with the TD-DFT value ($f = 0.0057$) is excellent. The experimental values have uncertainties of 20%, primarily due to the uncertainty in the decay rate of $v_{\text{TiO}} = 0$; thus, the level of agreement with the calculated result is likely accidental. Fluorescence dominates the excited state decay rate for the $v_{\text{TiO}} = 0$ band. This suggests that bare TiO^+ (²Π) is likely to fluoresce, which provides a route for its characterization in laboratory studies.

Current spectroscopic information on TiO^+ is from photoelectron spectroscopy of TiO by Dyke et al.⁴⁵ and Sappéy et al.⁴⁶ They agree on the ground ²Δ state of TiO^+ . Dyke et al. also observe a band at $T_0 = 10 250 \pm 80$ cm⁻¹ with $\omega_e = 860 \pm 60$ cm⁻¹ and $r_e = 1.73 \pm 0.01$ Å, which they assign to the A, ²Σ⁺ state.⁴⁵ Sappéy et al. observe an excited ²Σ⁺ state with $T_0 = 11 227 \pm 17$ cm⁻¹, $\omega_e = 1020 \pm 9$ cm⁻¹, and anharmonicity $\omega_e x_e = 6 \pm 2$ cm⁻¹.⁴⁶ Although this state lies at a similar energy to the ²Σ state observed by Dyke et al., the very different vibrational frequencies led Sappéy et al. to propose that TiO^+ has two low-lying ²Σ states, and resonant two-photon ionization reaches one state, while one-photon ionization accesses another. Our photodissociation study of $\text{TiO}^+(\text{CO}_2)$ probes the ²Π state of TiO^+ . This state has the electron configuration ...8σ², 3π⁴, 4π¹ and thus cannot be reached by simply removing an electron from neutral TiO, so it was not observed by Dyke et al. The multiphoton ionization study of Sappéy et al. used several intermediate electronic states of TiO, so they could conceivably ionize to the ²Π state of TiO^+ , but

their study did not extend to sufficiently high energies. However, our calculations shed light on the $^2\Sigma$ states observed by photoelectron spectroscopy. The TD-DFT calculations predict *one* low-lying $^2\Sigma$ state of TiO^+ , at $T_0 = 11\,403\text{ cm}^{-1}$ with $\omega_e = 1131\text{ cm}^{-1}$, $\omega_e x_e = 5\text{ cm}^{-1}$, and $r_e = 1.55\text{ \AA}$. These values are in excellent agreement with the values for the $^2\Sigma$ state observed by Sappey et al. The next $^2\Sigma$ state is predicted to lie at much higher energy, with $T_e = 30\,600\text{ cm}^{-1}$. It is not clear why the one-photon photoelectron study of TiO gives such a low vibrational frequency for the A $^2\Sigma$ state of TiO^+ . One possibility is that the high temperature ($\sim 800\text{ K}$) of the molecules and modest spectral resolution lead to overlapping vibrational bands that are easily mis-assigned.

Neutral TiO has been detected near numerous stars based on absorption in three strong electronic transitions in the visible.^{28–30} The resulting rotational, vibrational, and spin-orbit structure is used to measure the local temperature.^{31,32} The low ionization energy of TiO and high bond strength of TiO^+ make it likely that TiO^+ is also present in circumstellar envelopes. The electronic spectrum of TiO^+ has not been measured, which clearly hampers its detection. Optical transitions from the $^2\Delta$ ground state to the low-lying $^2\Sigma$ state of TiO^+ identified in the photoelectron spectroscopy of TiO are forbidden. The high $\text{Ti}^+ - \text{O}$ bond strength¹⁷ of 664 kJ/mol also makes it difficult to characterize via photofragment spectroscopy. We can combine our calculations on TiO^+ and $\text{TiO}^+(\text{CO}_2)$ and experimental results on $\text{TiO}^+(\text{CO}_2)$ to predict the electronic spectroscopy of bare TiO^+ . The calculations indicate that binding to CO_2 affects the $^2\Pi$ state of TiO^+ : lowering ω_e by 16 cm^{-1} and T_e by 1508 cm^{-1} . For $\text{TiO}^+(\text{CO}_2)$, we measure $T_0 = 13\,918\text{ cm}^{-1}$ and $\omega'_{\text{TiO}} = 952\text{ cm}^{-1}$ with anharmonicity $x'_{\text{TiO}} = 5\text{ cm}^{-1}$. We would then predict that the $^2\Pi$ state of TiO^+ has $\omega_e = 968 \pm 5\text{ cm}^{-1}$ with anharmonicity $\omega_e x_e = 5\text{ cm}^{-1}$ and lies at $T_0 = 15\,426 \pm 200\text{ cm}^{-1}$. The estimated value of T_0 ignores differences in zero-point energy in vibrations other than the Ti–O stretch between the two states. These values are very close to recent very high level multireference calculations by Miliordos and Mavridis.⁵⁸ At the TD-DFT level, the $^2\Pi - ^2\Delta$ transition in bare TiO^+ is calculated to have an integrated oscillator strength $f = 0.0050$. At the same level of theory, the strong $\alpha(^3\Delta - ^3\Delta)$ and $\gamma(^3\Phi - ^3\Delta)$ transitions in neutral TiO are calculated to each have $f \approx 0.11$, in accord with higher level calculations.²⁸ The relative weakness of the $^2\Pi - ^2\Delta$ band in TiO^+ will make its circumstellar detection challenging. Astronomical searches for TiO^+ will require accurate transition frequencies, and these values provide an excellent starting point for laboratory studies of TiO^+ , perhaps by sensitive techniques such as cavity ring-down spectroscopy or laser-induced fluorescence.

IV. Conclusions

Photofragment spectroscopy of $\text{TiO}^+(\text{CO}_2)$ has been used to characterize the $^2A''$ ($^2\Pi$) excited state. Photoexcited $\text{TiO}^+(\text{CO}_2)$ shows a wide range of excited state lifetimes, which is likely due to slow internal conversion at lower energies. Reduced intensity in the $\nu_{\text{TiO}} = 0$ band in the photodissociation spectrum is consistent with the low photodissociation quantum yield due to competition with fluorescence. From the measured excited state lifetimes and relative band intensities, the fluorescence rate is calculated to be $k_{\text{fl}} = 7.5 \times 10^5\text{ s}^{-1}$. This corresponds to an integrated oscillator strength of $f = 0.0056$. The experimental band origin and Ti–O stretching frequency of $\text{TiO}^+(\text{CO}_2)$, along with calculations on TiO^+ and $\text{TiO}^+(\text{CO}_2)$, allow for the prediction of the excitation energy and vibrational frequency of the $^2\Pi$ state of bare TiO^+ .

Acknowledgment. The authors thank E. Miliordos and A. Mavridis for providing their ab initio results on TiO^+ prior to publication. Financial support from the National Science Foundation under award CHE-0608446 is gratefully acknowledged.

References and Notes

- Centi, G.; Cavani, F.; Trifirò, F. *Selective Oxidation by Heterogeneous Catalysis*; Kluwer Academic: New York, 2001.
- Hadjivanov, K. I.; Klissurski, D. G. *Chem. Soc. Rev.* **1996**, *25*, 61.
- Yu, W.; Freas, R. B. *J. Am. Chem. Soc.* **1990**, *112*, 7126.
- Guo, B. C.; Kerns, K. P.; Castleman, A. W., Jr. *Int. J. Mass Spectrom. Ion Process.* **1992**, *117*, 129.
- Liu, X. H.; Zhang, X. G.; Li, Y.; Wang, X. Y.; Lou, N. Q. *Int. J. Mass Spectrom.* **1998**, *177*, L1.
- Harvey, J. N.; Diefenbach, M.; Schröder, D.; Schwarz, H. *Int. J. Mass Spectrom.* **1999**, *182*, 85.
- Schröder, D.; Schwarz, H. *Angew. Chem., Int. Ed. Engl.* **1995**, *34*, 1973.
- Schröder, D.; Schwarz, H.; Clemmer, D. E.; Chen, Y.; Armentrout, P. B.; Baranov, V.; Böhme, D. K. *Int. J. Mass Spectrom. Ion Process.* **1997**, *161*, 175.
- Schröder, D.; Schwarz, H.; Shaik, S. *Struct. Bonding (Berlin)* **2000**, *97*, 91.
- Böhme, D. K.; Schwarz, H. *Angew. Chem., Int. Ed. Engl.* **2005**, *44*, 2336.
- Chen, Y.-M.; Clemmer, D. E.; Armentrout, P. B. *J. Phys. Chem.* **1994**, *98*, 11490.
- MacTaylor, R. S.; Vann, W. D.; Castleman, A. W., Jr. *J. Phys. Chem.* **1996**, *100*, 5329.
- Cheng, P.; Koyanagi, G. K.; Böhme, D. K. *J. Phys. Chem. A* **2007**, *111*, 8561.
- Koyanagi, G. K.; Böhme, D. K. *J. Phys. Chem. A* **2006**, *110*, 1232.
- Herman, J.; Foutch, J. D.; Davico, G. E. *J. Phys. Chem. A* **2007**, *111*, 2461.
- Clemmer, D. E.; Elkind, J. L.; Aristov, N.; Armentrout, P. B. *J. Chem. Phys.* **1991**, *95*, 3387.
- Armentrout, P. B.; Kickel, B. L. Gas-Phase Thermochemistry of Transition Metal Ligand Systems: Reassessment of Values and Periodic Trends. In *Organometallic Ion Chemistry*; Freiser, B. S., Ed.; Kluwer Academic Publishers: Dordrecht, The Netherlands, 1994; p 1.
- Bellert, D.; Buthelezi, T.; Brucat, P. J. *Chem. Phys. Lett.* **1998**, *290*, 316.
- Asher, R. L.; Bellert, D.; Buthelezi, T.; Brucat, P. J. *Chem. Phys. Lett.* **1994**, *227*, 623.
- Asher, R. L.; Bellert, D.; Buthelezi, T.; Weerasekera, G.; Brucat, P. J. *Chem. Phys. Lett.* **1994**, *228*, 390.
- Citir, M.; Altinay, G.; Metz, R. B. *J. Phys. Chem. A* **2006**, *110*, 5051.
- Citir, M.; Metz, R. B. *J. Chem. Phys.* **2008**, *128*, 024307.
- Gregoire, G.; Duncan, M. A. *J. Chem. Phys.* **2002**, *117*, 2120.
- Duncan, M. A. *Int. Rev. Phys. Chem.* **2003**, *22*, 407.
- Walker, N. R.; Walters, R. S.; Grieves, G. A.; Duncan, M. A. *J. Chem. Phys.* **2004**, *121*, 10498.
- Walker, N. R.; Walters, R. S.; Duncan, M. A. *J. Chem. Phys.* **2004**, *120*, 10037.
- Bellert, D.; Buthelezi, T.; Hayes, T.; Brucat, P. J. *Chem. Phys. Lett.* **1997**, *276*, 242.
- Langhoff, S. R. *Astrophys. J.* **1997**, *481*, 1007.
- Allard, F.; Hauschildt, P. H.; Schwenke, D. *Astrophys. J.* **2000**, *540*, 1005.
- Morgan, W. W.; Keenan, P. C. *Ann. Rev. Astron. Astrophys.* **1973**, *11*, 29.
- Kotnik-Karuzza, D.; Jurdana-Sepic, R. *Astron. Astrophys.* **2000**, *355*, 595.
- Couch, P. A.; Evans, T. L.; Sarre, P. J. *Mon. Not. R. Astron. Soc.* **2003**, *346*, 153.
- Matsuoka, L.; Hasegawa, S. *J. Opt. Soc. Am. B* **2007**, *24*, 2562.
- Lo, H. H.; Fite, W. L. *Chem. Phys. Lett.* **1974**, *29*, 39.
- Schofield, K. *J. Phys. Chem. A* **2006**, *110*, 6938.
- Petrie, S.; Böhme, D. K. *Astrophys. J.* **1994**, *436*, 411.
- Oppenheimer, M.; Dalgarno, A. *Astrophys. J.* **1977**, *212*, 683.
- Petrie, S.; Böhme, D. K. *Mass Spectrom. Rev.* **2007**, *26*, 258.
- Merer, A. J. *Annu. Rev. Phys. Chem.* **1989**, *40*, 407.
- Ram, R. S.; Bernath, P. F.; Dulick, M.; Wallace, L. *Astrophys. J. Supp. Ser.* **1999**, *122*, 331.
- Kobayashi, K.; Hall, G. E.; Muckerman, J. T.; Sears, T. J.; Merer, A. J. *J. Mol. Spectrosc.* **2002**, *212*, 133.
- Virgo, W. L.; Steimle, T. C.; Brown, J. M. *Astrophys. J.* **2005**, *628*, 567.

- (43) Namiki, K.; Saito, S.; Robinson, J. S.; Steimle, T. C. *J. Mol. Spectrosc.* **1998**, *191*, 176.
- (44) Harrison, J. F. *Chem. Rev.* **2000**, *100*, 679.
- (45) Dyke, J. M.; Gravenor, B. W. J.; Josland, G. D.; Lewis, R. A.; Morris, A. *Mol. Phys.* **1984**, *53*, 465.
- (46) Sappey, A. D.; Eiden, G.; Harrington, J. E.; Weisshaar, J. C. *J. Chem. Phys.* **1989**, *90*, 1415.
- (47) Looock, H. P.; Simard, B.; Wallin, S.; Linton, C. *J. Chem. Phys.* **1998**, *109*, 8980.
- (48) Husband, J.; Aguirre, F.; Ferguson, P.; Metz, R. B. *J. Chem. Phys.* **1999**, *111*, 1433.
- (49) Metz, R. B. *Int. Rev. Phys. Chem.* **2004**, *23*, 79.
- (50) Metz, R. B. *Adv. Chem. Phys.* **2008**, *138*, 331.
- (51) Thompson, C. J.; Faherty, K. P.; Stringer, K. L.; Metz, R. B. *Phys. Chem. Chem. Phys.* **2005**, *7*, 814.
- (52) Frisch, M. J.; Trucks, G. W.; Schlegel, H. B.; Scuseria, G. E.; Robb, M. A.; Cheeseman, J. R.; Montgomery, J. A., Jr.; Vreven, T.; Kudin, K. N.; Burant, J. C.; Millam, J. M.; Iyengar, S. S.; Tomasi, J.; Barone, V.; Mennucci, B.; Cossi, M.; Scalmani, G.; Rega, N.; Petersson, G. A.; Nakatsuji, H.; Hada, M.; Ehara, M.; Toyota, K.; Fukuda, R.; Hasegawa, J.; Ishida, M.; Nakajima, T.; Honda, Y.; Kitao, O.; Nakai, H.; Klene, M.; Li, X.; Knox, J. E.; Hratchian, H. P.; Cross, J. B.; Adamo, C.; Jaramillo, J.; Gomperts, R.; Stratmann, R. E.; Yazyev, O.; Austin, A. J.; Cammi, R.; Pomelli, C.; Ochterski, J. W.; Ayala, P. Y.; Morokuma, K.; Voth, G. A.; Salvador, P.; Dannenberg, J. J.; Zakrzewski, V. G.; Dapprich, S.; Daniels, A. D.; Strain, M. C.; Farkas, O.; Malick, D. K.; Rabuck, A. D.; Raghavachari, K.; Foresman, J. B.; Ortiz, J. V.; Cui, Q.; Baboul, A. G.; Clifford, S.; Cioslowski, J.; Stefanov, B. B.; Liu, G.; Liashenko, A.; Piskorz, P.; Komaromi, I.; Martin, R. L.; Fox, D. J.; Keith, T.; Al-Laham, M. A.; Peng, C. Y.; Nanayakkara, A.; Challacombe, M.; Gill, P. M. W.; Johnson, B.; Chen, W.; Wong, M. W.; Gonzalez, C.; Pople, J. A. *Gaussian 03*; Gaussian, Inc.: Wallingford, CT, Pittsburgh PA, 2004.
- (53) Nakao, Y.; Hirao, K.; Taketsugu, T. *J. Chem. Phys.* **2001**, *114*, 7935.
- (54) Gutsev, G. L.; Andrews, L.; Bauschlicher, C. W., Jr. *Theor. Chem. Acc.* **2003**, *109*, 298.
- (55) Irigoras, A.; Fowler, J. E.; Ugalde, J. M. *J. Phys. Chem. A* **1998**, *102*, 293.
- (56) Sodupe, M.; Branchadell, V.; Rosi, M.; Bauschlicher, C. W., Jr. *J. Phys. Chem. A* **1997**, *101*, 7854.
- (57) McLaughlin, B. M.; Ballance, C. P.; Berrington, K. A. *J. Phys. B: At. Mol. Opt. Phys.* **2001**, *34*, L179.
- (58) Miliordos, E.; Mavridis, A. Personal communication.
- (59) Miliordos, E.; Mavridis, A. *J. Phys. Chem. A* **2007**, *111*, 1953.
- (60) Aguirre, F.; Husband, J.; Thompson, C. J.; Stringer, K. L.; Metz, R. B. *J. Chem. Phys.* **2003**, *119*, 10194.

JP809648C